



Effect of chloride and sulfate additions on corrosion of low alloy steel in high-temperature water



Konsta Sipilä^a, Martin Bojinov^{b,1,*}, Wolfgang Mayinger^c, Timo Saario^a, Michael Stanislowski^c

^aVTT Materials and Building, VTT Technical Research Centre of Finland, P.O. Box 1000, FIN-02044 Espoo, Finland

^bDepartment of Physical Chemistry, University of Chemical Technology and Metallurgy, 1756 Sofia, Bulgaria

^cE.ON Kernkraft GmbH, Tresckowstraße 5, 30457 Hannover, Germany

ARTICLE INFO

Article history:

Received 26 February 2015

Received in revised form 8 April 2015

Accepted 23 May 2015

Available online 27 May 2015

Keywords:

low-alloyed steel

high-temperature water

chloride and sulfate additions

impedance spectroscopy

kinetic model

ABSTRACT

The present paper investigates the effect of chloride and sulfate additions on corrosion of low-alloyed steel in a cladding flaw of a nuclear reactor pressure vessel using in-situ electrochemical impedance spectroscopy coupled to ex-situ characterization of the oxides by surface analytical techniques. Impedance data are interpreted by the mixed-conduction model for oxide films to yield estimates for the main kinetic and transport parameters of the corrosion process. It can be concluded that the effect of chloride/sulfate transients on low-alloyed steel oxides is moderate, concerns mostly the processes at the inner layer/coolant interface and is to a certain extent reversible.

©2015 Elsevier Ltd. All rights reserved.

1. Introduction

In light water reactors, the pressure vessel and in some cases also the piping is made of low-alloyed steel (LAS), covered with a welded stainless steel cladding for improved corrosion protection. In structural failure assessments of primary circuits, penetrating cladding flaws that could locally expose the underlying LAS to the coolant are assumed. Due to the narrow opening of such weld defects, the aqueous solution in contact with the LAS is expected to have a different composition, and thus be more aggressive towards the structural material when compared to the bulk coolant.

Strain-induced corrosion cracking (SICC) in LAS has been extensively investigated during the last decades [1–28]. As a result, the following environmental parameters have been observed to affect the initiation and growth of SICC: temperature, flow rate, redox potential, dissolved oxygen content, as well as impurities such as Cl^- , SO_4^{2-} and H_2S . One important finding from recent laboratory investigations [18,21–24,26] is the observed detrimental role of small amounts of chloride and sulfate anions, which has been shown to increase the cracking susceptibility of LAS even at constant load. Although boiling water reactors (BWRs) are usually

operated with neutral high purity water, increased transient levels of sulfate and chloride >5 ppb may occur during start-up and occasionally during steady-state power operation, due to ion exchanger resin intrusions or condenser leakages [21].

Crack initiation is often assumed to involve changes of the surface films at the electrolyte/LAS interface in the modified crevice solution in the cladding flaw. Thus investigating the oxide film properties in such environments is a plausible approach towards understanding crack initiation. In that context, the aim of the present investigation is twofold: first, to estimate the prevailing chemical and electrochemical conditions at the LAS/coolant interface in a cladding flaw with chloride and sulfate present, and second, to carry out an experimental study of the effect of chloride, sulfate and sulfate + chloride concentration transients in such occluded chemistry conditions on the electrical and electrochemical properties, the thickness, composition and structure of the oxide films formed on low-alloyed steels.

2. Chemical and electrochemical conditions in a cladding flaw

In order to investigate the effect of impurities on the corrosion behavior of LAS, the chemical and electrochemical conditions in a cladding flaw are first estimated by using a mixed-potential model for the corrosion reactions of stainless steel walls and low-alloyed steel bottom. The model is coupled to equations describing the transport of all the ionic and neutral species in the flaw electrolyte,

* Corresponding author. Tel.: +359 889 298 679; fax: +359 2 868 20 36.

E-mail addresses: martin@uctm.edu, mbojinov@yahoo.com (M. Bojinov).

¹ ISE member

Nomenclature

a_{Fe}	rate of Fe oxidation at $E=0$ V; $A\ m^{-2}$
a	rate of proton reduction at $E=0$ V; $A\ m^{-2}$
a_{H_2O}	rate of water reduction at $E=0$ V; $A\ m^{-2}$
a_{H_2}	rate of hydrogen oxidation at $E=0$ V; $A\ m^{-2}$
a_O	rate of oxygen reduction at $E=0$ V and oxygen concentration of $1\ mol\ m^{-3}$; $A\ mol^{-0.66}$
c_i	concentration of a soluble species (Eq. (1)), $mol\ m^{-3}$
C	space-charge layer capacitance of the semiconductor phase in the inner layer, $\mu F\ cm^{-2}$
$C_{F/E}$	double-layer capacitance at the inner layer/water interface, $\mu F\ cm^{-2}$
D_e	diffusivity of electronic defects, $cm^2\ s^{-1}$ (assumed to be equal to 10^{-8})
D_i	diffusivity of aqueous species at 561 K, $cm^2\ s^{-1}$ (Table 2)
D_O	diffusivity of oxygen vacancies, $cm^2\ s^{-1}$
\bar{E}	field strength in the inner layer, $V\ cm^{-1}$
K_i	equilibrium constant of a homogeneous reaction (Eqs. (2)–(7))
L	thickness of the inner layer, cm
k_1	rate constant of the iron oxidation reaction at the steel/inner layer interface, $mol\ cm^{-2}\ s^{-1}$
k_2	rate constant of oxygen incorporation at the inner layer/water interface, $cm\ s^{-1}$
R_i	rate of a homogeneous reaction, $mol\ m^{-3}\ s^{-1}$
R_{el}	uncompensated electrolyte resistance between the samples, $\Omega\ cm^2$
$R_{F/E}$	charge transfer resistance of the redox reaction at the inner layer/water interface, $\Omega\ cm^2$
R_t	charge transfer resistance at the steel/inner layer interface, $\Omega\ cm^2$
α	part of the potential consumed at the inner layer/water interface
α_{Fe}	transfer coefficient of iron oxidation
α_H	transfer coefficient of proton and water reduction
α_{H_2}	transfer coefficient of hydrogen oxidation
α_O	transfer coefficient of oxygen reduction
ϵ	dielectric constant of the inner layer (assumed to be equal to 12)

treated as a dilute electrolyte solution. As a result of the calculations, estimates of the most aggressive conditions in terms of chloride and sulfate enrichment factors in the crevice are obtained.

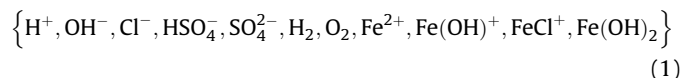
2.1. Cladding flaw geometry

The system geometry is illustrated in Fig. 1. It is important to mention that the interfaces 2 and 3 extend to the bulk solution and thus no out-flux of species to the external surfaces adjacent to the

flaw opening are expected. Due to the different reactions occurring at the interfaces 2 and 3 (cladding flaw solution/stainless steel) and 4 (cladding flaw solution/ low-alloyed steel), 2D simulations are used and discussed below. The dimension in the third direction is presumed to be much larger compared to the other two, and can thus be considered infinite.

2.2. Chemical species

Following the approach described in references [29–32], the set of species that define the chemical environment is



Thus a total of 12 species (including of course water) is taken as representative for the cladding flaw environment in contact with low-alloyed steel. Concerning the possibility of reduction of sulfate and hydrosulfate to sulfide and/or hydrosulfide (H_2S and HS^-), preliminary thermodynamic calculations gave indications that especially at high SO_4 concentrations, such reactions are possible. At this stage of the investigation, however, they have not been taken into account due to the lack of reliable information on their kinetics in high-temperature water. Experimental determination of the kinetics of sulfate reduction is planned to be performed in the near future. In order to simulate the effect of Cr in the solution phase, also the chromium cation, chromium hydroxide and chloride complexes need to be added. However, chromium will be present only as Cr(III) in the conditions under study since thermodynamic calculations show that the oxidation potential for Cr(III) to Cr(VI) is much higher than the typical redox potential in de-oxygenated high-temperature water at 561 K.

2.3. Homogeneous chemical reactions

The species considered are linked by the following homogeneous reactions

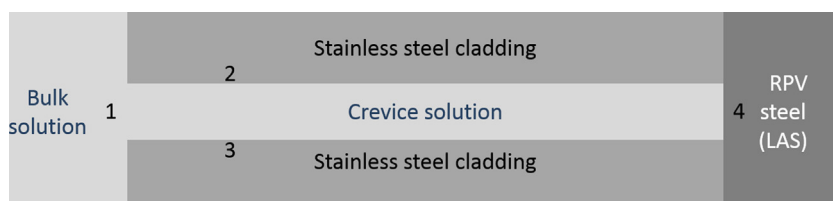
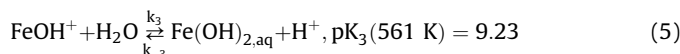
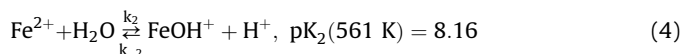
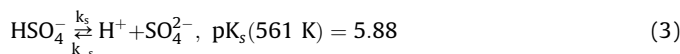
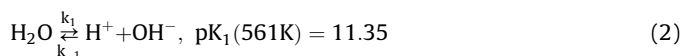


Fig. 1. Crevice geometry considered in the present approach.

Download English Version:

<https://daneshyari.com/en/article/183846>

Download Persian Version:

<https://daneshyari.com/article/183846>

[Daneshyari.com](https://daneshyari.com)